Analytic formula for the proton radioactivity spectroscopic factor

Dong-Meng Zhang,[1] Lin-Jing Qi,[1] Hai-Feng Gui,[1] Song Luo,[1] Biao He,[2,*] Xi-Jun Wu,[3,†] and Xiao-Hua Li[1,4,5,‡]

[1]*School of Nuclear Science and Technology, University of South China, 421001 Hengyang, People's Republic of China*

[2]*College of Physics and Electronics, Central South University, Changsha 410083, People's Republic of China*

[3]*School of Math and Physics, University of South China, Hengyang 421001, People's Republic of China*

[4]*Cooperative Innovation Center for Nuclear Fuel Cycle Technology & Equipment, University of South China, 421001 Hengyang, People's Republic of China*

[5]*National Exemplary Base for International Science & Technology Collaboration of Nuclear Energy and Nuclear Safety, University of South China, Hengyang 421001, People's Republic of China*

(Received 14 April 2023; revised 20 June 2023; accepted 9 August 2023; published 22 August 2023)

In the present work, we systematically study the spectroscopic factor of proton radioactivity (S_p) with $A > 100$ using the deformed two-potential approach (D-TPA). It is found that there is a link between the quadrupole deformation parameter of proton emitter and S_p. Based on this result, we propose a simple analytic formula for estimating the spectroscopic factor of proton radioactivity. With the help of this formula, the calculated half-lives of proton radioactivity can reproduce the experimental data successfully within a factor of 2.77. Furthermore, we extend the D-TPA with this formula for evaluating the spectroscopic factor to predict the proton radioactivity half-lives of 12 proton radioactivity candidates whose radioactivity is energetically allowed or observed but not yet quantified in NUBASE2020. For comparison, the universal decay law for proton radioactivity (UDLP) and the new Geiger-Nuttall law (NG-N) are also used. It turns out that all of the predicted results are basically consistent with each other.

DOI: 10.1103/PhysRevC.108.024318

I. INTRODUCTION

One of the most important decay modes for proton-rich nuclide far away from the β-stability line is proton radioactivity, which is a quantum-tunneling effect [1]. Studying proton radioactivity half-lives may be of great importance in promoting the existing nuclear theories and/or models, describing nuclear deformation, and understanding the decay properties of nuclei [2–9]. The first confirmation for proton radioactivity was obtained by Jackson *et al.* in the measurement of an isomeric state for ^{53}Co [10,11]. In 1981, at the velocity filter SHIP at GSI, Hofmann *et al.* first discovered the proton emission from nuclear ground state of ^{151}Lu [12]. Subsequently, the proton emitter ^{147}Tm was discovered in an experiment performed at GSI [13], and ^{109}I and ^{113}Cs were observed using a catcher foil technique at Munich [14]. In 1984, Hofmann *et al.* discovered the isomeric decay in ^{147}Tm and the ground decay of ^{150}Lu [15]. The highly deformed proton emitters ^{141}Ho and ^{131}Eu were reported by Davids *et al.* in subsequent years [16]. In addition to the above decay processes, with the advancement of diverse infrastructures and radioactive beam installations, a number of proton emitters have been confidently identified in recent decades in the proton region $51 < Z < 83$ from the ground state or low-lying isomeric state [17,18].

To date, proton radioactivity has become one of the most popular topics in the field of nuclear physics [2,3,6,19]. Moreover, study of the spectroscopic factor of proton radioactivity (S_p) may facilitate the investigation of nuclear structures such as nuclear deformation [20,21] and quantum mixing [22]. In theory, S_p can be regarded as a probability that the blocked proton in the orbit of the parent nucleus would transfer to the empty orbit of the daughter nucleus. There are many microscopical theories to estimate it, including the relativistic mean field theory (RMF) with the Bardeen-Cooper-Schriffer (BCS) theory [4,20,23–25], relativistic continuum Hartree-Bogoliubov (RCHB) theory [26], covariant density functional (CDF) with BCS [27], etc. Phenomenologically, S_p can be obtained by the ratio of the theoretical proton radioactivity half-life to experimental data [28]. Besides, in the numerous calculations, S_p is generally assumed to be a constant [5,17], which causes the omission of microscopic information about the nuclear structure.

Recently, Chen *et al.* [28] proposed a simple analytic formula for the spectroscopic factor of spherical proton emitters with the same orbital angular momentum l. However, this formula is unsuitable for the well deformed proton emitters. In 2021, Delion *et al.* discovered that there is a small residual linear decrease of the logarithm of the spectroscopic factor versus the quadrupole deformation parameter of proton emitters [29]. As a result, a new perspective is to propose a unified definition of the spectroscopic factor for spherical and

*hbinfor@163.com
†wuxijun1980@yahoo.cn
‡lixiaohuaphysics@126.com

deformed proton emitters. To account for this, we establish a connection between the spectroscopic factor and the deformation parameter employing the deformed two-potential approach (D-TPA). The results suggest that S_p can be expressed as a formula involving the quadrupole deformation parameter of proton emitters. This formula can be utilized for estimating the spectroscopic factor and conducting accurate calculations of proton radioactivity half-lives.

This article is organized as follows. In Sec. II, the theoretical framework of D-TPA is introduced in detail. The results and discussion are presented in Sec. III. Finally, a brief summary is given in Sec. IV.

II. THEORETICAL FRAMEWORK

The proton radioactivity half-life $T_{1/2}$ is correlated with the decay width Γ. It can be expressed as

$$T_{1/2} = \frac{\hbar \ln 2}{\Gamma}, \tag{1}$$

where $\hbar$ represents the reduced Planck constant. In the framework of two-potential approach (TPA) [28,30,31], Γ can be determined by the normalized factor F and penetration probability P, and expressed as

$$\Gamma = S_p \frac{\hbar^2 F P}{4\mu}, \tag{2}$$

where S_p is the spectroscopic factor of the emitted proton-daughter system. In the present work, S_p is assumed as a constant, i.e., $S_p = 1$, which is crucial for the subsequent systematic analysis. $\mu = mA_d/(A_d + A_p)$ MeV/c^2 is the reduced mass of the emitted proton-daughter nucleus system, where m is the nucleon mass. A_p and A_d are the mass numbers of the emitted proton and daughter nucleus, respectively.

F represents the normalized factor, which describes the emitted proton assault frequency as it passes through the potential barrier. Taking into account the effect of deformation, we can obtain the total normalized factor F by averaging F_θ over all possible orientations. It can be expressed as

$$F = \frac{1}{2}\int_0^\pi F_\theta \sin\theta \, d\theta, \tag{3}$$

where θ is the orientation angle of the emitted proton measured from the symmetry axis of the daughter nucleus, and F_θ can be written as

$$F_\theta = \frac{1}{\int_{r_1}^{r_2} \frac{1}{2k(r,\theta)} dr}. \tag{4}$$

P, the penetration probability for the emitted proton penetrating the barrier, can be obtained by the semiclassical Wentzel-Kramers-Brillouin (WKB) approximation. Considering the effect of deformation, we can obtain the total penetration probability P by averaging P_θ in all directions. It can be written as

$$P = \frac{1}{2}\int_0^\pi P_\theta \sin\theta \, d\theta, \tag{5}$$

where the polar-angle-dependent penetration probability of proton radioactivity, P_θ, is given by

$$P_\theta = \exp\left[-2\int_{r_2}^{r_3} k(r,\theta) dr\right]. \tag{6}$$

Here $k(r,\theta) = \sqrt{\frac{2\mu}{\hbar^2}|V(r,\theta) - Q_p|}$ is the wave number. $V(r,\theta)$ is the total interaction potential between the emitted proton and daughter nucleus. In Eqs. (4) and (6), r_1, r_2, and r_3 represent the classical turning points, which satisfy the condition $V(r,\theta) = Q_p$. The proton radioactivity released energy Q_p can be obtained by

$$Q_p = \Delta M - (\Delta M_d + \Delta M_p) + k(Z^\varepsilon - Z_d^\varepsilon), \tag{7}$$

where ΔM, ΔM_d, and ΔM_p represent the mass excesses of parent and daughter nuclei and the emitted proton, respectively. They are taken from the latest atomic mass table NUBASE2020 [32]. The term $k(Z^\varepsilon - Z_d^\varepsilon)$ denotes the screening effect of atomic electrons with $k = 13.6$ eV, $\varepsilon = 2.408$ for $Z < 60$, and $k = 8.7$ eV, $\varepsilon = 2.517$ for $Z \geqslant 60$ [33,34]. Here Z and Z_d are the proton numbers of parent nucleus and daughter nucleus, respectively.

In the present work, the total interaction potential $V(r,\theta)$ consists of the nuclear potential $V_N(r,\theta)$, Coulomb potential $V_C(r,\theta)$, and centrifugal potential $V_l(r)$. It can be expressed as

$$V(r,\theta) = V_N(r,\theta) + V_C(r,\theta) + V_l(r). \tag{8}$$

The emitted proton-daughter nucleus nuclear potential $V_N(r,\theta)$ is chosen as a type of cosh parametrized form [35]. It can be expressed as

$$V_N(r,\theta) = -V_0 \frac{1 + \cosh[R_d(\theta)/a]}{\cosh(r/a) + \cosh[R_d(\theta)/a]}, \tag{9}$$

where V_0 and a are the parameters of the depth and diffuseness of the nuclear potential, respectively. We choose $V_0 = 57.83$ MeV and $a = 0.857$ fm, which are taken from Ref. [30]. Taking into account the deformed effect of daughter nucleus,

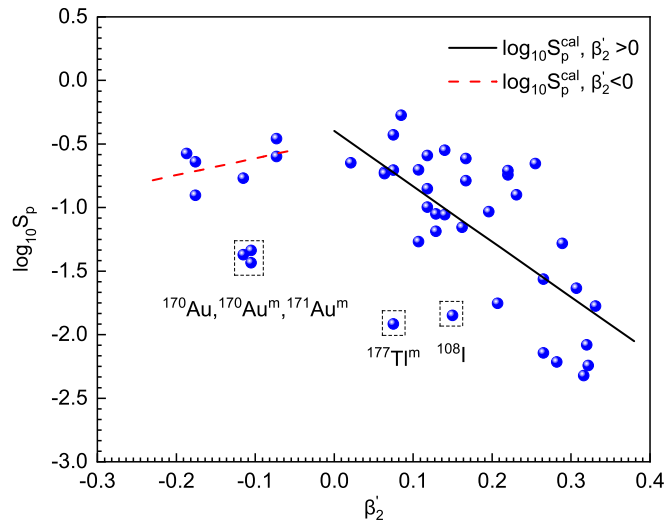

FIG. 1. The linear relationship between the logarithmic value of experimental spectroscopic factor, $\log_{10}S_p^{\rm exp}$, and β_2'.

TABLE I. Comparison of experimental proton radioactivity half-lives with the calculated ones by using different theoretical models and/or formulas. The symbol m denotes the first isomeric state. The experimental proton radioactivity half-lives, spin, and parity are taken from Ref. [32]. The released energies are given by Eq. (7) with the exception of Q_p values for ^{130}Eu, ^{159}Re, ^{161}Re^m, ^{164}Ir and ^{177}Tl^m taken from Ref. [3].

Nucleus	Q_p				$\log_{10} T_{1/2}$(s)				
$^A Z$	(MeV)	l	$S_p^{\exp}$	S_p^{cal}	Exp	Cal^1	Cal^2	UDLP [44]	NG-N [45]
^{108}I	0.610	2	0.014	0.089	0.723	−1.124	−0.073	−0.019	0.829
^{109}I	0.829	2	0.070	0.079	−4.032	−5.187	−4.084	−3.671	−3.157
^{112}Cs	0.820	2	0.093	0.056	−3.310	−4.341	−3.090	−2.923	−2.362
^{113}Cs	0.981	2	0.018	0.050	−4.771	−6.542	−5.224	−4.899	−4.490
^{117}La	0.831	2	0.006	0.024	−1.664	−3.878	−2.252	−2.459	−1.857
^{121}Pr	0.901	2	0.005	0.017	−1.921	−4.241	−2.468	−2.811	−2.237
^{130}Eu	1.039	2	0.021	0.014	−3.000	−4.776	−2.936	−3.357	-2.789
^{131}Eu	0.963	2	0.008	0.016	−1.699	−3.777	−1.986	−2.458	−1.840
^{135}Tb	1.203	3	0.006	0.016	−2.996	−5.235	−3.437	−3.806	−3.212
^{140}Ho	1.104	3	0.052	0.022	−2.222	−3.502	−1.846	−2.317	−1.600
^{141}Ho	1.194	3	0.007	0.028	−2.387	−4.528	−2.977	−3.257	−2.583
^{141}Ho^m	1.264	0	0.027	0.028	−5.137	−6.822	−5.147	−5.331	−5.524
^{144}Tm	1.724	5	0.222	0.031	−5.569	−6.194	−4.714	−4.687	−4.991
^{145}Tm	1.754	5	0.126	0.039	−5.499	−6.371	−4.994	−4.871	−5.182
^{146}Tm	0.904	0	0.181	0.044	−0.810	−1.551	−0.196	−0.610	−0.968
^{146}Tm^m	1.214	5	0.195	0.044	−1.137	−1.846	−0.490	−0.896	−0.737
^{147}Tm^m	1.133	2	0.267	0.187	−3.444	−4.017	−3.289	−2.859	−2.183
^{150}Lu	1.285	5	0.230	0.193	−1.347	−1.986	−1.272	−1.132	−0.965
^{150}Lu^m	1.305	2	0.125	0.193	−4.398	−5.298	−4.588	−4.050	−3.381
^{151}Lu	1.255	5	0.163	0.075	−0.896	−1.682	−0.558	−0.862	−0.653
^{151}Lu^m	1.315	2	0.244	0.075	−4.796	−5.408	−4.284	−4.150	−3.471
^{155}Ta	1.466	5	0.226	0.324	−2.495	−3.141	−2.652	−2.269	−2.161
^{156}Ta	1.036	2	0.252	0.265	−0.826	−1.424	−0.848	−0.624	0.102
^{156}Ta^m	1.126	5	0.349	0.265	0.933	0.476	1.053	0.947	1.371
^{157}Ta	0.946	0	0.534	0.171	−0.527	−0.800	−0.032	−0.038	−0.363
^{159}Re	1.816	5	0.190	0.211	−4.678	−5.400	−4.721	−4.270	−4.285
^{159}Re^m	1.816	5	0.185	0.211	−4.665	−5.398	−4.721	−4.269	−4.283
^{160}Re	1.276	2	0.199	0.137	−3.163	−3.865	−3.001	−2.841	−2.101
^{161}Re	1.216	0	0.258	0.123	−3.357	−3.945	−3.034	−2.895	−3.018
^{161}Re^m	1.338	5	0.141	0.123	−0.678	−1.528	−0.616	−0.806	−0.501
^{164}Ir	1.844	5	0.054	0.137	−3.947	−5.213	−4.351	−4.114	−4.039
^{165}Ir^m	1.727	5	0.101	0.123	−3.433	−4.427	−3.515	−3.408	−3.266
^{166}Ir	1.167	2	0.065	0.110	−0.824	−2.009	−1.050	−1.188	−0.426
^{166}Ir^m	1.347	5	0.089	0.110	−0.076	−1.126	−0.166	−0.475	−0.100
^{167}Ir	1.087	0	0.283	0.098	−1.120	−1.668	−0.661	−0.865	−1.076
^{167}Ir^m	1.262	5	0.088	0.098	0.842	−0.214	0.794	0.348	0.798
^{170}Au	1.487	2	0.037	0.241	−3.487	−4.920	−4.302	−3.845	−3.023
^{170}Au^m	1.767	5	0.046	0.241	−2.971	−4.307	−3.688	−3.333	−3.118
^{171}Au	1.464	0	0.170	0.233	−4.652	−5.425	−4.788	−4.298	−4.228
^{171}Au^m	1.718	5	0.043	0.233	−2.587	−3.957	−3.324	−3.026	−2.777
^{176}Tl	1.278	0	0.198	0.189	−2.208	−2.912	−2.187	−2.059	−2.113
^{177}Tl	1.173	0	0.375	0.189	−1.174	−1.600	−0.876	−0.875	−1.015
^{177}Tl^m	1.967	5	0.012	0.189	−3.346	−5.260	−4.535	−4.227	−3.972
^{185}Bi^m	1.625	0	0.023	0.018	−4.191	−5.838	−4.090	−4.759	−4.511

$R_d(\theta)$ is given by [36]

$$R_d(\theta) = R'_d(1 + \beta_2 Y_{20}(\theta) + \beta_4 Y_{40}(\theta) + \beta_6 Y_{60}(\theta)), \quad (10)$$

where β_2, β_4, and β_6 denote the quadrupole, hexadecapole, and hexacontatetrapole deformation parameters of the residual daughter nucleus, which are taken from FRDM2012 (finite-range droplet model) tables [37]. $Y_{lm}(\theta)$ is a spherical harmonics function. R'_d is the spherical radius of daughter nucleus [38], which can be expressed as

$$R'_d = 1.27 A_d^{1/3}. \quad (11)$$

Based on the double folding model, the Coulomb potential for the deformed daughter and emitted proton can be

expressed as [39]

$$V_C(\vec{r},\theta) = \iint \frac{\rho_d(\vec{r}_1)\rho_p(\vec{r}_2)}{|\vec{r}+\vec{r}_1+\vec{r}_2|} d\vec{r}_1 d\vec{r}_2, \tag{12}$$

where $\vec{r}$ is the vector between the centers of the emitter proton and daughter nucleus. Meanwhile, $\vec{r}_1$ and $\vec{r}_2$ represent the radius vectors in the charge distributions of the emitter proton and daughter nucleus, respectively. $\rho_d(\vec{r}_1)$ and $\rho_p(\vec{r}_2)$ denote the charge density distribution of the deformed daughter nucleus and spherical emitted proton, respectively. Simplified by the Fourier transform, the Coulomb potential can be presented as [39–41]

$$V_C(\vec{r},\theta) = V_C^{(0)}(\vec{r},\theta) + V_C^{(1)}(\vec{r},\theta) + V_C^{(2)}(\vec{r},\theta), \tag{13}$$

where $V_C^{(0)}(\vec{r},\theta)$, $V_C^{(1)}(\vec{r},\theta)$, and $V_C^{(2)}(\vec{r},\theta)$ are the bare Coulomb interaction, linear Coulomb coupling, and second-order Coulomb coupling, respectively. The specific expressions of $V_C^{(0)}(\vec{r},\theta)$, $V_C^{(1)}(\vec{r},\theta)$, and $V_C^{(2)}(\vec{r},\theta)$ are presented in Ref. [31].

For the centrifugal potential $V_l(r)$, we adopt the Langer modified form, since the correction $l(l+1) \to (l+1/2)^2$ is essential for one-dimension problems [42]. It can be expressed as

$$V_l(r) = \frac{\hbar^2\left(l+\frac{1}{2}\right)^2}{2\mu r^2}. \tag{14}$$

Here l is the angular momentum taken away by the emitted proton, which satisfies the spin-parity conservation laws. It can be expressed as

$$l = \begin{cases} \Delta_j & \text{for even } \Delta_j \text{ and } \pi = \pi_d, \\ \Delta_j + 1 & \text{for even } \Delta_j \text{ and } \pi \neq \pi_d, \\ \Delta_j & \text{for odd } \Delta_j \text{ and } \pi \neq \pi_d, \\ \Delta_j + 1 & \text{for odd } \Delta_j \text{ and } \pi = \pi_d, \end{cases} \tag{15}$$

where $\Delta_j = |j - j_d - j_p|$ with j, π, j_d, π_d, and j_p, π_p denoting the spin and parity values of the parent nucleus, daughter nucleus and the emitted proton, respectively.

III. RESULTS AND DISCUSSION

In our previous work [31], we used the D-TPA to study the effect of daughter deformation on half-life of α decay. Considering that proton radioactivity shares the same mechanism as α decay, in this work we try to extend this model to describe proton radioactivity. First, based on the D-TPA, we calculate the proton radioactivity half-lives with $S_p = 1$ for proton emitters in the ground state as well as in the isomeric state. Using the ratio of the calculated proton radioactivity half-life $T_{1/2}^{\rm cal}$ to the experimental one $T_{1/2}^{\rm exp}$, it is possible to determine the experimental spectroscopic factor ($S_p^{\rm exp}$), which is defined as $S_p^{\rm exp} = T_{1/2}^{\rm cal}/T_{1/2}^{\rm exp}$. A comparison between experimental and theoretical spectroscopic factors shows a good consistency between them, with the exception of rare cases where the experimental data are below the theoretical predictions [43]. These differences in behavior are due to the influence of nuclear structure effects such as deformation and quantum mixing that are not taken into account in simple calculations [22]. In other words, the spectroscopic factor may be dependent on deformation in the microscopic model adopted for calculating the proton radioactivity half-lives. Recently, Delion *et al.* discovered that there is a small residual linear decrease of the spectroscopic factor in logarithmic form versus the quadrupole deformation parameter of proton emitters (β_2') [29]. In that regard, we consider establishing the correlation between extracted experimental spectroscopic factors and β_2'. Adopting the extracted experimental spectroscopic factor in logarithmic form, $\log_{10}S_p^{\rm exp}$ as a function of β_2' is plotted in Fig. 1. From this figure, it is worth noting that there are five points which clearly deviate from the fitting line, corresponding to particular nuclei ^{108}I, ^{170}Au, ^{170}Au^m, ^{171}Au^m and ^{177}Tl^m. The large discrepancies and small $S_p^{\rm exp}$ values occur at $Z = 79$ and 81, maybe due to the strong proton shell effect. Particularly, the emitted protons are all from the $\pi h_{11/2}$ state

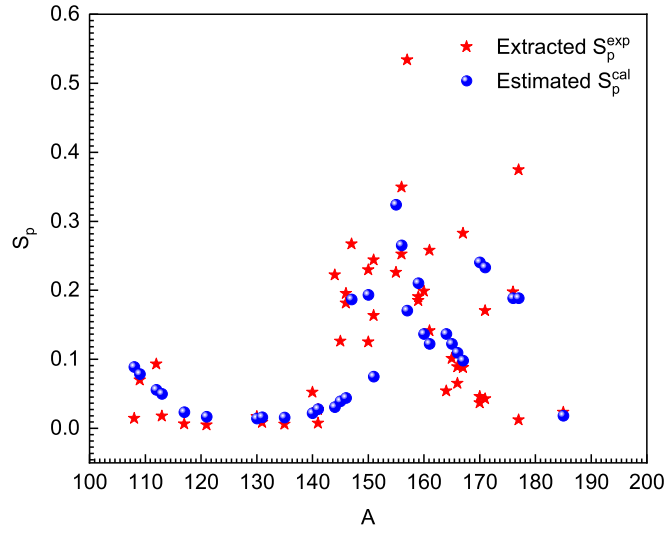

FIG. 2. The experimental spectroscopic factor $S_p^{\rm exp}$ and the calculated one by Eq. (16) of deformed proton emitters.

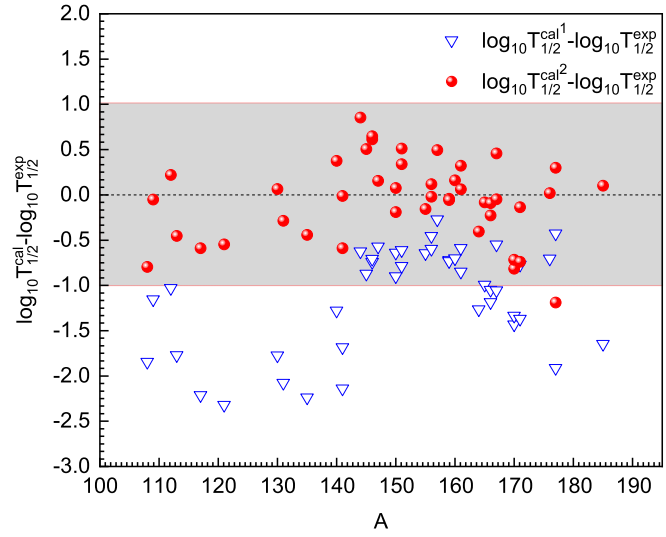

FIG. 3. Deviations between the experimental proton radioactivity half-lives and two calculated ones for deformed nuclei.

TABLE II. Standard deviations σ between experimental half-lives and the calculated ones using different theoretical models and/or formulas.

Type	Cal[1]	Cal[2]	UDLP	NG-N
σ	1.253	0.443	0.478	0.516

for $^{171}\mathrm{Au}^{m}$ and $^{177}\mathrm{Tl}^{m}$, corresponding to the orbit of shell closure in the shell model picture [20]. Similarly, the proton number of ^{108}I is close to the magic number $Z = 50$, and the proton shell effect may be a reason for this phenomenon. On the whole, we can clearly see that there is an obvious linear relationship between the experimental spectroscopic factor in logarithmic form, $\log_{10}S_p^{\mathrm{exp}}$, and β_2'. Then, a simple formula is put forward for evaluating the spectroscopic factor of proton radioactivity as

$$\log_{10}S_p = \begin{cases} a\beta_2' + b & \text{for } \beta_2' > 0, \\ c\beta_2' + d & \text{for } \beta_2' < 0, \end{cases} \tag{16}$$

where the parameters $a = -4.353$, $b = -0.398$, $c = 1.332$, and $d = -0.479$ are determined by fitting the extracted experimental spectroscopic factor data. In the following, we adopt Eq. (16) to calculate the spectroscopic factors, denoted as S_p^{cal}. In order to visually exhibit the agreement between the experimental spectroscopic factors S_p^{exp} and calculated ones S_p^{cal}, they are plotted as red stars and solid blue circles in Fig. 2, respectively. From this figure, we can distinctly see that S_p^{cal} can fit S_p^{exp} well, which indicates that the simple analytic formula for estimating the spectroscopic factor is credible.

Furthermore, based on the D-TPA, we calculate the half-lives of proton radioactivity with the spectroscopic factors taken as 1 and obtained by Eq. (16). For comparison, the universal decay law for proton radioactivity (UDLP) [44] and the new Geiger-Nuttall law (NG-N) [45] are also used. All predicted results are listed in Table I. In this table, the first five columns represent proton emitters, the released energy of proton radioactivity, Q_p, the angular momentum l taken away by the emitted proton, extracted experimental spectroscopic factor S_p^{exp}, and calculated spectroscopic factor S_p^{cal}, respectively. The last five columns denote the logarithmic form of the experimental proton radioactivity half-lives and theoretical ones calculated using the D-TPA with S_p taken as 1 and S_p obtained by Eq. (16), UDLP, and NG-N, which are denoted as Cal[1], Cal[2], UDLP, and NG-N. As shown in Table I, after considering the spectroscopic factors S_p^{cal} obtained by Eq. (16), calculated proton radioactivity half-lives Cal[2] can well reproduce experimental data in the region of 10^{-5} to 10^{2} s. For clarity, the deviations between the experimental proton radioactivity half-lives and the calculated ones, $\log_{10}T_{1/2}^{\mathrm{cal}^1}$ and $\log_{10}T_{1/2}^{\mathrm{cal}^2}$, are plotted in Fig. 3. From this figure, we can clearly see that the $\log_{10}T_{1/2}^{\mathrm{cal}^1}$ are obviously lower than experimental data over the entire region corresponding to the deviations between -2.5 and 0. The reason for large deviations caused by $S_p = 1$ may be that the influence of deformation on spectroscopic factor is not taken into account. Particularly, the deviations are near zero as well as within ± 1 when the spectroscopic factors obtained by Eq. (16) are considered, indicating that $\log_{10}T_{1/2}^{\mathrm{cal}^2}$ can better reproduce experimental data. It explains the correlation between the spectroscopic factor and the deformation effect from a certain point of view and further validates the reliability of our formula.

In order to gain a global insight into the agreement between experimental data and the calculated ones, the standard σ is used to quantify the calculated capabilities of the above models and/or formulas. It can be defined as

$$\sigma = \sqrt{\frac{1}{N}\sum_{i=1}^{N}\left(\log_{10}T_{1/2}^{\mathrm{cal}.i} - \log_{10}T_{1/2}^{\mathrm{exp}.i}\right)^2}, \tag{17}$$

where $\log_{10}T_{1/2}^{\mathrm{cal}.i}$ and $\log_{10}T_{1/2}^{\mathrm{exp}.i}$ denote the experimental proton radioactivity half-life and the calculated one in logarithmic

TABLE III. Comparison of the predicted half-lives for possible radioactivity candidates whose proton radioactivity is energetically allowed or observed but not yet quantified in NUBASE2020. The symbol m denotes the first isomeric state. The released energies of proton radioactivity are given by Eq. (7).

Nucleus	Q_p			$\log_{10}T_{1/2}$(s)			
^{A}Z	(MeV)	l	S_p^{cal}	Cal[1]	Cal[2]	UDLP [44]	NG-N [45]
^{103}Sb	0.979	2	0.324	–7.732	–7.243	–5.948	–5.698
^{111}Cs	1.740	2	0.063	–12.292	–11.088	–10.094	–10.145
^{116}La	1.591	2	0.026	–11.117	–9.539	–9.000	–8.887
^{127}Pm	0.792	2	0.015	–1.761	0.069	–0.620	0.094
^{159}Re	1.606	0	0.211	–7.614	–6.937	–6.227	–6.156
^{162}Re	0.760	2	0.110	4.388	5.348	4.597	5.322
^{165}Ir	1.547	0	0.123	–6.662	–5.750	–5.387	–5.303
$^{169}\mathrm{Ir}^{m}$	0.782	5	0.088	7.638	8.692	7.362	8.363
^{169}Au	1.947	0	0.241	–9.027	–8.408	–7.572	–7.276
^{172}Au	0.877	2	0.123	3.319	4.231	3.578	4.284
^{184}Bi	1.330	0	0.018	–2.949	–1.215	–2.144	–2.123
^{185}Bi	1.541	5	0.018	–1.568	0.167	–1.030	–0.508

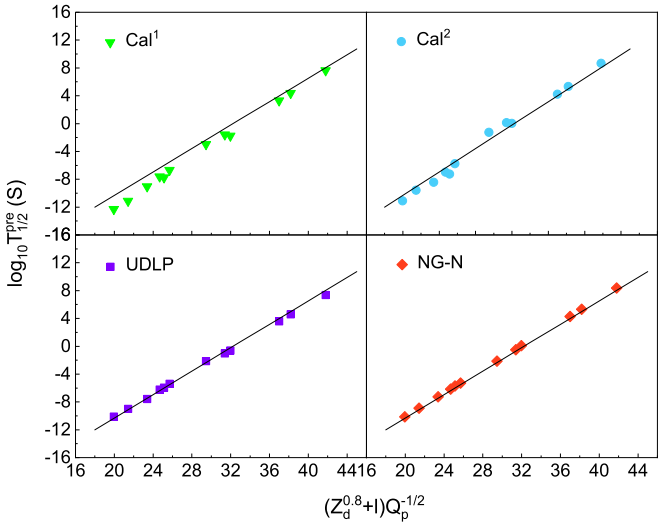

FIG. 4. Relationship between the predicted results of these models and/or formulas listed in Table III and Coulomb parameters considering the effect of the orbital angular momentum, i.e., NG-N [45].

form for the i-th nucleus, respectively. For comparison, all the specific results of σ are listed in Table II, which shows that $\sigma_{\mathrm{Cal}^1} = 1.253$, $\sigma_{\mathrm{Cal}^2} = 0.443$, $\sigma_{\mathrm{UDLP}} = 0.478$, and $\sigma_{\mathrm{NG\text{-}N}} = 0.516$. These results indicate that there is indeed some improvement after considering the spectroscopic factor. The spectroscopic factor of proton radioactivity can be simply described by a formula of β_2'. Besides, we can see that $\sigma_{\mathrm{Cal}^2} = 0.443$ is smaller than the ones calculated by the UDLP and NG-N, which are reduced by 7.32% and 14.15%.

Given the good agreement between the calculated results with the experimental data, based on the D-TPA, we use the present formula to estimate the spectroscopic factors and predict half-lives of 12 possible proton emitters whose radioactivity is energetically allowed or observed but not quantified in NUBASE2020 [32]. For comparison, the UDLP and NG-N are also used. The detailed predictions are listed in Table III. In this table, the first four columns represent the possible proton radioactivity candidates, released energy Q_p, orbital angular momentum l, and calculated spectroscopic factors S_p^{cal}, respectively. The next two columns represent the calculated proton radioactivity half-lives obtained by our model with $S_p = 1$ and after considering the spectroscopic factor in logarithmic form, denoted as Cal^1 and Cal^2, respectively. The last two columns are the predicted proton radioactivity half-lives using UDLP and NG-N. Noting from this table, the predicted proton radioactivity half-lives using our model are reasonably consistent with the ones using the other two formulas. Moreover, to further compare the evaluation capabilities of the above approaches, the relationship between the predicted results of these four models and/or formulas and Coulomb parameters considering the effect of the orbital angular momentum, i.e., NG-N, is plotted in Fig. 4. The results show that all predictions are basically consistent with the NG-N, which means our predictions of the proton radioactivity half-lives are valid and reliable. These predictions may provide valuable information for seeking new nuclides with proton radioactivity.

IV. SUMMARY

In summary, for evaluating the spectroscopic factor of proton radioactivity, we propose a simple analytic expression for describing the relationship between the spectroscopic factor extracted from the experimental proton radioactivity half-life and the quantity β_2'. The present formula for the spectroscopic factor can be successfully applied to estimate the spectroscopic factors as well as calculate half-lives. As an application, we extend this model to predict proton radioactivity half-lives for 12 possible candidates. The predicted results are in great agreement with other ones obtained by UDLP and NG-N. This work may provide useful and reliable information for experimental and theoretical research in the future.

ACKNOWLEDGMENTS

This work is supported in part by the National Natural Science Foundation of China (Grants No. 12175100 and No. 11975132), the construct program of the key discipline in Hunan province, the Research Foundation of Education Bureau of Hunan Province, China (Grant No. 18A237), the Shandong Province Natural Science Foundation, China (Grant No. ZR2022JQ04), the Opening Project of Cooperative Innovation Center for Nuclear Fuel Cycle Technology and Equipment, University of South China (Grant No. 2019KFZ10), and the Innovation Group of Nuclear and Particle Physics in USC, Hunan Provincial Innovation Foundation for Postgraduate (Grant No. CX20210942).

[1] C. Xu and Z. Ren, Phys. Rev. C **73**, 041301(R) (2006).
[2] D. S. Delion, R. J. Liotta, and R. Wyss, Phys. Rev. Lett. **96**, 072501 (2006).
[3] B. Blank and M. J. G. Borge, Prog. Part. Nucl. Phys. **60**, 403 (2008).
[4] H. F. Zhang, Y. J. Wang, J. M. Dong, J. Q. Li, and W. Scheid, J. Phys. G: Nucl. Part. Phys. **37**, 085107 (2010).
[5] J. L. Chen, X. H. Li, J. H. Cheng, J. G. Deng, and X. J. Wu, J. Phys. G: Nucl. Part. Phys. **46**, 065107 (2019).
[6] D. S. Delion, Phys. Rev. C **80**, 024310 (2009).
[7] M. Karny, K. Rykaczewski, R. Grzywacz, J. Batchelder, C. Bingham, C. Goodin, C. Gross, J. Hamilton, A. Korgul, W. Królas *et al.*, Phys. Lett. B **664**, 52 (2008).
[8] Z. X. Zhang and J. M. Dong, Chin. Phys. C **42**, 014104 (2018).
[9] D. N. Basu, P. R. Chowdhury, and C. Samanta, Phys. Rev. C **72**, 051601(R) (2005).
[10] K. P. Jackson, C. U. Cardinal, H. C. Evans, N. A. Jelley, and J. Cerny, Phys. Lett. B **33**, 281 (1970).

[11] J. Cerny, J. Esterl, R. Gough, and R. Sextro, Phys. Lett. B **33**, 284 (1970).
[12] S. Hofmann, W. Reisdorf, G. Münzenberg, F. P. Heßberger, J. R. H. Schneider, and P. Armbruster, Z. Phys. A **305**, 111 (1982).
[13] O. Klepper, T. Batsch, S. Hofmann, R. Kirchner, W. Kurcewicz, W. Reisdorf, E. Roeckl, D. Schardt, and G. Nyman, Z. Phys. A **305**, 125 (1982).
[14] T. Faestermann, A. Gillitzer, K. Hartel, P. Kienle, and E. Nolte, Phys. Lett. B **137**, 23 (1984).
[15] S. Hofmann, in *Proceedings of the 7th International Conference on Atomic Masses Fundamental Constants*, edited by O. Klepper, THD-Schriftenreihe Wissenschaft und Technik Vol. 26 (GSI, Darmstadt, 1984), p. 184.
[16] C. N. Davids, P. J. Woods, D. Seweryniak, A. A. Sonzogni, J. C. Batchelder, C. R. Bingham, T. Davinson, D. J. Henderson, R. J. Irvine, G. L. Poli, J. Uusitalo, and W. B. Walters, Phys. Rev. Lett. **80**, 1849 (1998).
[17] K. P. Santhosh and I. Sukumaran, Pramana-J. Phys. **92**, 6 (2019).
[18] H. F. Zhang, Y. Z. Wang, J. M. Dong, and J. Q. Li, Sci. China Ser. G-Phys. Mech. Astron. **52**, 1536 (2009).
[19] Y. Z. Wang, J. P. Cui, Y. H. Gao, and J. Z. Gu, Commun. Theor. Phys. **73**, 075301 (2021).
[20] Y. B. Qian and Z. Z. Ren, Eur. Phys. J. A **52**, 68 (2016).
[21] L. S. Ferreira, E. Maglione, and D. E. P. Fernandes, Phys. Rev. C **65**, 024323 (2002).
[22] P. J. Woods and C. N. Davids, Annu. Rev. Nucl. Part. Sci. **47**, 541 (1997).
[23] J. M. Dong, H. F. Zhang, and G. Royer, Phys. Rev. C **79**, 054330 (2009).
[24] D. S. Delion, R. J. Liotta, and R. Wyss, Phys. Rep. **424**, 113 (2006).
[25] A. Soylu, F. Koyuncu, G. Gangopadhyay, V. Dehghani, and S. A. Alavi, Chin. Phys. C **45**, 044108 (2021).
[26] Y. Lim, X. Xia, and Y. Kim, Phys. Rev. C **93**, 014314 (2016).
[27] Q. Zhao, J. M. Dong, J. L. Song, and W. H. Long, Phys. Rev. C **90**, 054326 (2014).
[28] J. L. Chen, X. H. Li, X. J. Wu, P. C. Chu, and B. He, Eur. Phys. J. A **57**, 305 (2021).
[29] D. S. Delion and A. Dumitrescu, Phys. Rev. C **103**, 054325 (2021).
[30] J. H. Cheng, Y. Li, and T. P. Yu, Phys. Rev. C **105**, 024312 (2022).
[31] H. F. Gui, H. M. Liu, X. J. Wu, P. C. Chu, B. He, and X. H. Li, Commun. Theor. Phys. **74**, 055301 (2022).
[32] F. G. Kondev, M. Wang, W. J. Huang, S. Naimi, and G. Audi, Chin. Phys. C **45**, 030001 (2021).
[33] V. Y. Denisov and H. Ikezoe, Phys. Rev. C **72**, 064613 (2005).
[34] K. N. Huang, M. Aoyagi, M. H. Chen, B. Crasemann, and H. Mark, At. Data Nucl. Data Tables **18**, 243 (1976).
[35] B. Buck, A. C. Merchant, and S. M. Perez, Phys. Rev. C **45**, 2247 (1992).
[36] M. Ismail, W. M. Seif, A. Adel, and A. Abdurrahman, Nucl. Phys. A **958**, 202 (2017).
[37] P. Möller, A. J. Sierk, T. Ichikawa, and H. Sagawa, At. Data Nucl. Data Tables **109**, 1 (2016).
[38] N. Wang and W. Scheid, Phys. Rev. C **78**, 014607 (2008).
[39] N. Takigawa, T. Rumin, and N. Ihara, Phys. Rev. C **61**, 044607 (2000).
[40] M. Ismail, W. M. Seif, and H. El-Gebaly, Phys. Lett. B **563**, 53-6 (2003).
[41] G.-L. Zhang, X.-Y. Le, and Z.-H. Liu, Chin. Phys. Lett. **25**, 1247 (2008).
[42] J. J. Morehead, J. Math. Phys. **36**, 5431 (1995).
[43] S. Åberg, P. B. Semmes, and W. Nazarewicz, Phys. Rev. C **56**, 1762 (1997).
[44] C. Qi, D. S. Delion, R. J. Liotta, and R. Wyss, Phys. Rev. C **85**, 011303(R) (2012).
[45] J. L. Chen, J. Y. Xu, J. G. Deng, X. H. Li, B. He, and P. C. Chu, Eur. Phys. J. A **55**, 214 (2019).